PCCP

Accepted Manuscript

ROYAL SOCIETY OF CHEMISTRY

www.rsc.org/pccp

Eutectic melting of $LiBH_4$ – KBH_4

Morten B. Ley,[a] *Elsa Roedern,*[a] *Torben R. Jensen*[a]*

[a] Center for Materials Crystallography, Interdisciplinary Nanoscience Center (iNANO) and Department of Chemistry, University of Aarhus, Langelandsgade 140, DK-8000 Århus C, Denmark

* To whom correspondence should be addressed.

Torben R. Jensen, dr. scient., Associate Professor
Head of HyFillFast (project funded by DSF EnMi)
Center for Materials Crystallography (DGF)
iNANO and Department of Chemistry
Langelandsgade 140
DK-8000 Aarhus C
Aarhus University
Denmark
Phone: +45 87155939
mobile: +45 2272 1486
E-mail: trj@chem.au.dk

TOC figure

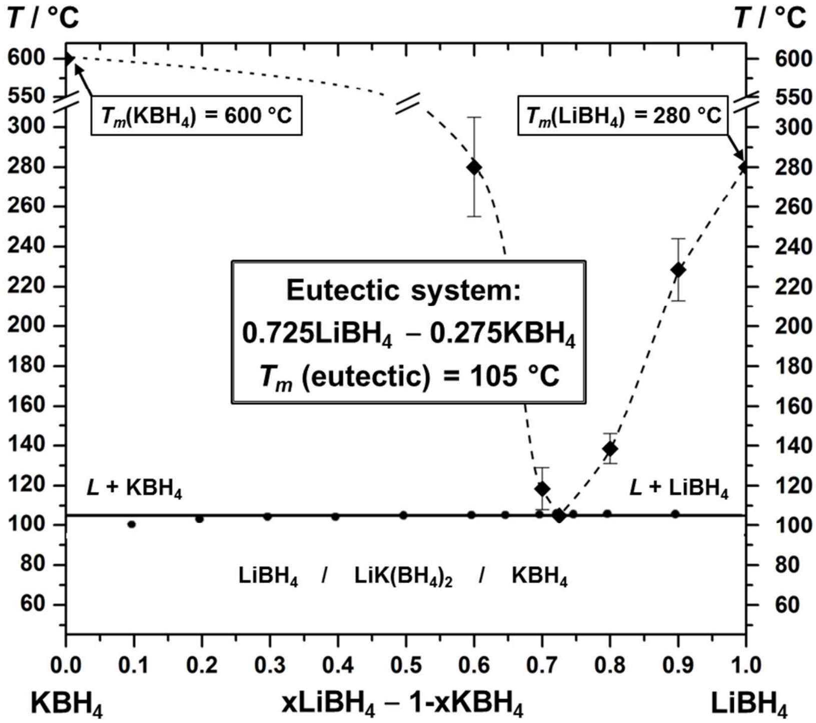

TOC text

Extremely low eutectic melting temperature, pressure stabilisation of a bi-metallic borohydride with implication for mechanochemistry

Abstract

Eutectic melting in mixtures of alkali and alkali earth metal borohydrides can pave the way for new applications as fast ionic conductors, facilitate hydrogen release by low temperature chemical reactions and convenient nanoconfinement. Here, we determine the eutectic composition for the lithium potassium borohydride system, $0.725LiBH_4$–$0.275KBH_4$, with the lowest melting point, $T_{\text{melt}} \sim 105$ ˚C, of all known alkali and alkali earth metal borohydride mixtures. Mechanochemistry and manual grounding of $LiBH_4$ and KBH_4 facilitates formation of $LiK(BH_4)_2$ from $LiBH_4$ – KBH_4 mixtures but not any of the melting or heat treatments used in this work. The bimetallic borohydride dissociates to the monometallic borohydrides at ~95 °C and partial melting occurs at ~105 °C. Analysis of the unit cell volumes of $LiBH_4$, KBH_4 and $LiK(BH_4)_2$ in the temperature range 25 to 90 °C indicate that formation of the bimetallic borohydride is facilitated by a more dense packing as compared to the reactants. Thus, $LiK(BH_4)_2$ is considered metastable and the formation pressure induced. A phase diagram for the $LiBH_4$–KBH_4 system is established, which illustrates the low eutectic melting point and the stability range for the bimetallic borohydride, $LiK(BH_4)_2$.

Keywords: Eutectic melting, Ionic liquid, Bimetallic borohydride, Lithium Potassium borohydride, Hydrogen storage.

Introduction

Renewable energy sources, e.g. sun and wind, fluctuate strongly over time and geographically, posing the challenge of efficient integration and reliable long-term energy storage.[1,2] A main focus is the development of an environmentally friendly successor for gasoline and hydrogen and Li-ion batteries are considered potential future carriers of renewable energy.[3–6] Hydrogen has the highest gravimetric energy density of all known substances, but low volumetric energy density and requires appropriate storage itself.[1] Metal borohydrides have very high hydrogen densities and significant structural flexibility, allowing for a range of new interesting properties such as Li-ion conductivity and luminescence.[7–12] Metal borohydrides as hydrogen storage materials often have poor thermodynamic and kinetic properties, which hamper in particular hydrogen uptake and their general utilisation in technological applications. Among the approaches towards improving these properties are nanoconfinement, cat- and anion substitution and structural processing.[13–15] Lately, the melting of metal borohydrides has received increased attention as a possible method for destabilising, release of hydrogen at lower temperatures and convenient preparation of nanoconfined materials. Metal borohydrides with low melting point may behave as ionic liquids and allow fast and convenient re-fuelling of vehicles with similar technology as known today for liquid fossil fuels. Ionic liquids receive significant interest for other properties as well, e.g. fast ion conductors, green chemistry or synthetic media.[16] Eutectic metal borohydrides are an alternative to hydrogen generation by hydrolysis reactions of aqueous solutions of e.g. sodium borohydride, which usually have relatively low hydrogen densities of 4-5 wt%.[3,17]

Mono-metallic borohydrides $M(BH_4)_x$, M = Li, Na, K, Mg or Ca, have high melting points, $T_m >$ 250 °C, but several eutectic melting bimetallic mixtures have been discovered, that have lower melting points compared to the individual metal borohydrides.[18–21] Thus, the lowest melting points reported for a eutectic bi-metal borohydride mixture is T_m = 180 °C for $xLiBH_4 – 1\text{-}xMg(BH_4)_2$, x =

0.5–0.6,[22–24] while $0.68LiBH_4$–$0.32Ca(BH_4)_2$ melts at 200 °C[25,26] and $0.62LiBH_4$–$0.38NaBH_4$ at 220 °C.[20,21] In the present study we conduct a systematic investigation of the $LiBH_4$–KBH_4 system and revisit the binary phase diagram.[19]

Methods

An overview of investigated samples and their method of preparation are given in Table 1. The samples were investigated by laboratory powder X-ray diffraction (PXD), *in situ* time resolved synchrotron radiation powder X-ray diffraction (SR-PXD), differential scanning calorimetry (DSC) and temperature programmed photographic analysis (TPPA). A detailed description of the sample preparation and characterisation methods is given in the electronic supplementary information (ESI).

Table 1 Overview of produced samples, synthesis and characterisation.

Sample	$xLiBH_4$	$1\text{-}xKBH_4$	Synthesis
s1	0.9	0.1	Hand mixing
s2	0.8	0.2	Hand mixing
s3	0.7	0.3	Hand mixing
s4	0.6	0.4	Hand mixing
s5	0.5	0.5	Hand mixing
s6	0.4	0.6	Hand mixing
s7	0.3	0.7	Hand mixing
s8	0.2	0.8	Hand mixing
s9	0.1	0.9	Hand mixing
s10	0.75	0.25	Hand mixing
s11	0.725	0.275	Hand mixing
s12	0.725	0.275	Ball milling, 240 min
s13	0.5	0.5	Ball milling, 36 h
s14	0.665	0.335	Ball milling, 36 h

Results & Discussion

Eutectic melting of $LiBH_4$ – KBH_4

Analysis of eutectic melting in all hand mixed samples **s1-s11** is performed using differential scanning calorimetry (DSC) and temperature programmed photographic analysis (TPPA) from room temperature (RT) to 300 °C. Lithium borohydride, $LiBH_4$, is known to undergo a phase transition from an orthorhombic (*o*) to a hexagonal (*h*) crystal system between 108 and 115 °C, depending on the heating rate and to melt at 275 °C.[27,28] The two observable and overlapping endothermic events during heating of $LiBH_4$−KBH_4 are therefore melting of the eutectic at 105 °C (onset temperature) and the *o*– to *h*–$LiBH_4$ polymorphic transition at ~113 °C in the samples with an excess of $LiBH_4$, see Figure 1B. The double peak or shoulder on the melting peak indicates an excess of $LiBH_4$ in the samples **s1**, **s2** and **s10**.

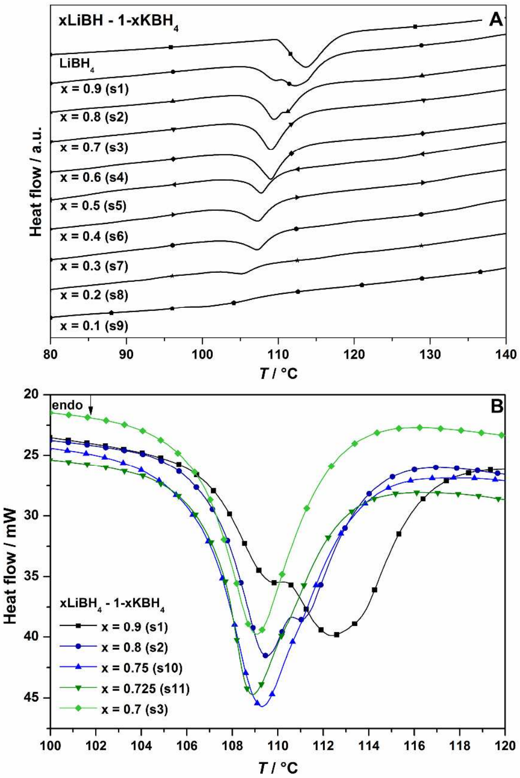

Figure 1 Differential scanning calorimetry data of $xLiBH_4$ – $1\text{-}xKBH_4$. **A)** Normalised DSC curves of $LiBH_4$ and **s1-s9** in the temperature range 80 to 140 °C. **B)** Selected DSC data of samples **s1-s3**, **s10**, **s11**.

The integrated area of the DSC peaks is proportional to the enthalpy of the thermal events, which cannot be separated during the integration.[26,29] The heat of reaction (dG) for the thermal events is extracted and plotted in **Figure 2** for the different sample compositions. The required energy for the endothermic event increases with increasing amounts of $LiBH_4$ and the highest value is obtained for **s11.**

The endothermic *o*– to *h*–$LiBH_4$ polymorphic transition accounts for 0.28 kJ/g or 6.2 kJ/mol in the sample with pure $LiBH_4$. This value lies between the previously reported 4.4 kJ/mol and the theoretically calculated 7.7 kJ/mol for the *o*– to *h*–$LiBH_4$ polymorphic transition.[30] The contribution of the polymorphic transition from the $LiBH_4$ fraction in the sample to the total heat of reaction is indicated in Figure 2, but since the polymorphic transition occurs at higher temperature than the melting, it is only relevant in samples with an excess of $LiBH_4$, as the already molten $LiBH_4$ does not undergo the polymorphic transition anymore. This causes the abrupt change in the heat of reaction between x = 7 and x = 7.25, indicating that the correct eutectic composition lies between $0.7LiBH_4$–$0.3KBH_4$ and $0.725LiBH_4$–$0.275KBH_4$.

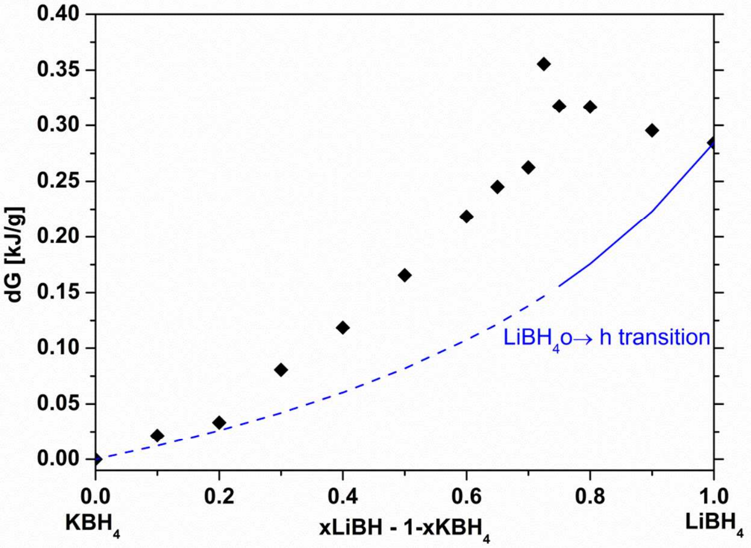

Figure 2 Integrated DSC signal in the temperature range 100 to 115 °C of the endothermic event per sample mass for KBH_4, s1-s11 and $LiBH_4$. Blue line: contribution of the *o*– to *h*–$LiBH_4$ polymorphic transition. However, since the phase transition only happens after the melting, this is only contributing in the samples with excess $LiBH_4$ (solid blue line)

Temperature programmed photographic analysis (TPPA) performed for the samples between room temperature and 300 °C confirms the observations from DSC, showing a complete melting of **s11** initiated at $T \sim 105$ °C. Selected pictures from TPPA for **s3**, **s10** and **s11** are shown in Figure 3, while pictures of **s1**, **s2** and **s4-s9** are presented in Figures S1-S8 (ESI). In the samples **s3**, **s10** and **s11,** partial melting is initiated at ~105 °C, at 120 °C the samples are completely molten and remain molten during further heating.

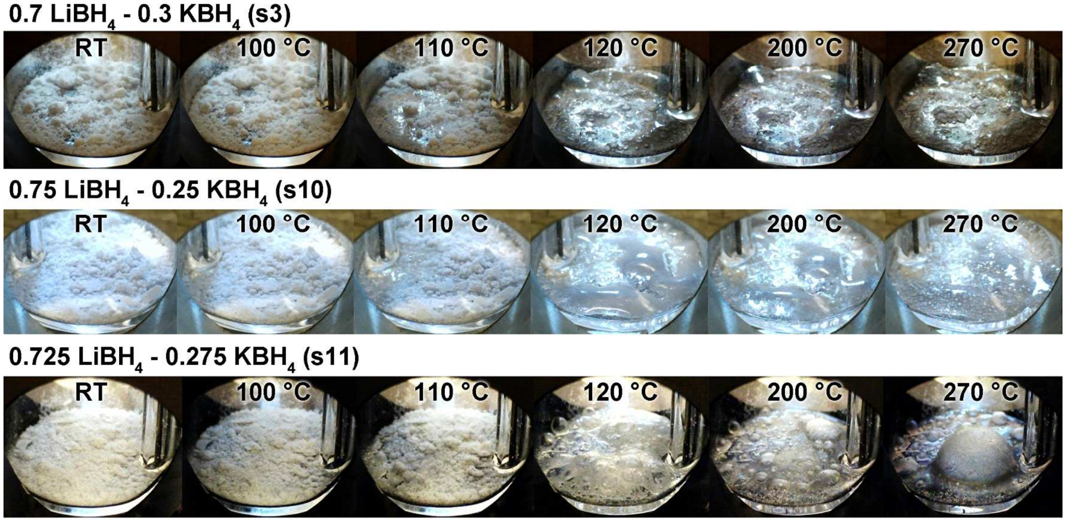

Figure 3 Temperature programmed photographic analysis of **s3, s10, s11** ($\Delta T/\Delta t = 5$ °C/min, argon atmosphere).

The melting in samples **s3**, **s10** and **s12**, was also studied by *in situ* time resolved synchrotron radiation powder X-ray diffraction (SR-PXD), see Figure 4, S9 and S10. $LiBH_4$, KBH_4 and $LiK(BH_4)_2$ are observed at RT in all three samples, demonstrating the readily formation of $LiK(BH_4)_2$ even by manual grounding in a mortar. The *in situ* SR-PXD experiments have not revealed any formation of solid solutions between $LiBH_4$ and KBH_4. The compounds either exist as separate phases or react to form the bimetallic compound $LiK(BH_4)_2$. Bragg peaks from $LiK(BH_4)_2$ disappear at ~95 °C associated with increasing diffracted intensity of $LiBH_4$ and KBH_4, which reveal that the bimetallic borohydride dissociate to the stable monometallic borohydrides. The (partial) melting at 105 °C is associated with a decrease of the intensity of the Bragg peaks from $LiBH_4$ and KBH_4. In sample **s3**, some KBH_4 remains crystalline until 150 °C (Figure S9), proving that the sample contains an excess of KBH_4 compared to the eutectic composition for the $LiBH_4$-KBH_4. The excess of $LiBH_4$ in sample **s10**, which was observed by DSC, is however not obvious by *in situ* SR-PXD after the melting (Figure S10).

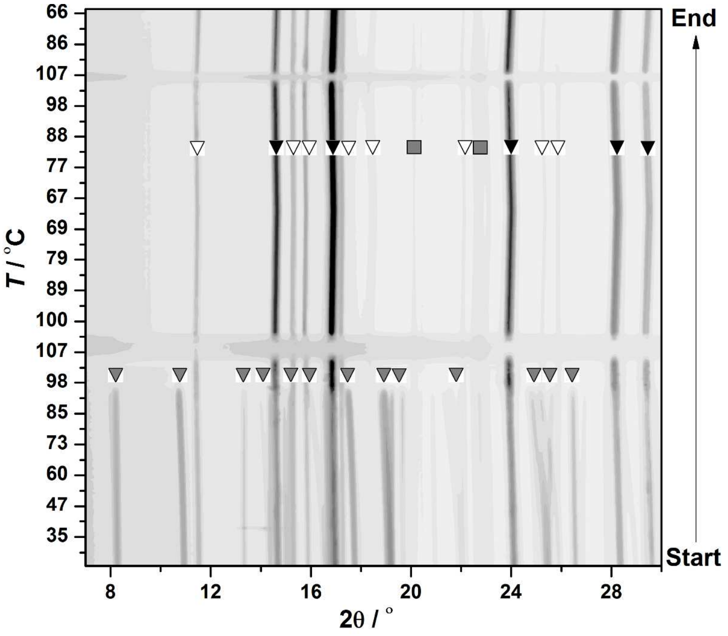

Figure 4 *In situ* SR-PXD heating-cooling experiment of $0.725LiBH_4$ – $0.275KBH_4$ (**s12**) from RT - 107 °C - 107 °C (2 min) - 65 °C – 107 °C - RT ($\Delta T/\Delta t = \pm 5$ °C/min, p(Ar) = 1 bar, $\lambda = 0.9919$ Å). Symbols: white triangle $LiBH_4$, black triangle KBH_4, grey triangle $LiK(BH_4)_2$ and grey square WC.

The reversible melting and resolidification of the eutectic composition $0.725LiBH_4$ – $0.275KBH_4$ (**s12**) was studied first by heating from RT to 107 °C followed by cooling to 65 °C and then heating again to 107 °C, before cooling to RT, see Figure 4 and a magnification of the first melting and solidification in Figure S11. At 105 °C, Bragg peaks from $LiBH_4$ and KBH_4 start to disappear and all diffraction vanish at 107 °C, which indicates that the sample is fully molten. This is also confirmed by an increase in the background intensity. After dwelling for 2 min at 107 °C, cooling is initiated and Bragg peaks from $LiBH_4$ and KBH_4 appear at 106 °C due to the crystallisation of the melt. During the second heating, Bragg peaks from $LiBH_4$ and KBH_4 again disappear simultaneously at 105 °C, accompanied by an increase in the background intensity. The Bragg peaks reappear during cooling at 104 °C revealing reversible eutectic melting of $0.725LiBH_4$ – $0.275KBH_4$ without formation of the bimetallic borohydride, $LiK(BH_4)_2$.

Binary phase diagram of $LiBH_4$–KBH_4

A summary of the comprehensive study of the temperature – composition relationships in the $LiBH_4$-KBH_4 binary system is illustrated as a binary phase diagram, Figure 5, which illustrate the eutectic melting of $0.725LiBH_4$–$0.275KBH_4$ at T = 105 °C and the phase separation of the bimetallic $LiK(BH_4)_2$ at T = 95 °C. The presence of $LiK(BH_4)_2$ in the samples is dependent on the preparation method, see next section. In all samples, no bimetallic $LiK(BH_4)_2$ was observed above T = 95 °C, however the dissociation of the metastable $LiK(BH_4)_2$ might occur at a lower temperatures over longer time due to slow kinetics of the separation.[31,32] The solidus temperatures were determined by DSC, however the decreasing melting point of the composite could not be detected by DSC unlike other eutectic borohydrides mixtures.[23,25] Instead, it was estimated by TPPA for samples **s1**-**s4**. The $LiBH_4$-KBH_4 system was first studied in the 1960s and 1970s, where melting was proposed to occur at T_m > 100 °C for KBH_4 rich mixtures, in disagreement with the results presented here.[19,20] However, these studies do not report any methods for determination of the melting point or details related to the sample preparation, which hampers comparison between the published data and the new results presented here. However, several other eutectic melting metal borohydrides contain excess $LiBH_4$, e.g. those based on $NaBH_4$, $Mg(BH_4)_2$ or $Ca(BH_4)_2$.[23,25] The LiCl–KCl system also has a eutectic composition, 0.58LiCl-0.42KCl, with a melting point of 361 °C. The melting points of LiCl and KCl are 610 and 772 °C, respectively, and in this system the eutectic composition also have a higher content of the lowest melting component (LiCl).[33] In a screening of a wide range of eutectically melting bimetallic borohydrides, preliminary experiments revealed partial melting at ~110 °C of $0.5LiBH_4$ – $0.5KBH_4$.[21] These considerations, the different independent techniques utilised here and the significant number of investigated samples all support that the eutectic composition of the lithium borohydride and potassium borohydride system is $0.725LiBH_4$-$0.275KBH_4$.

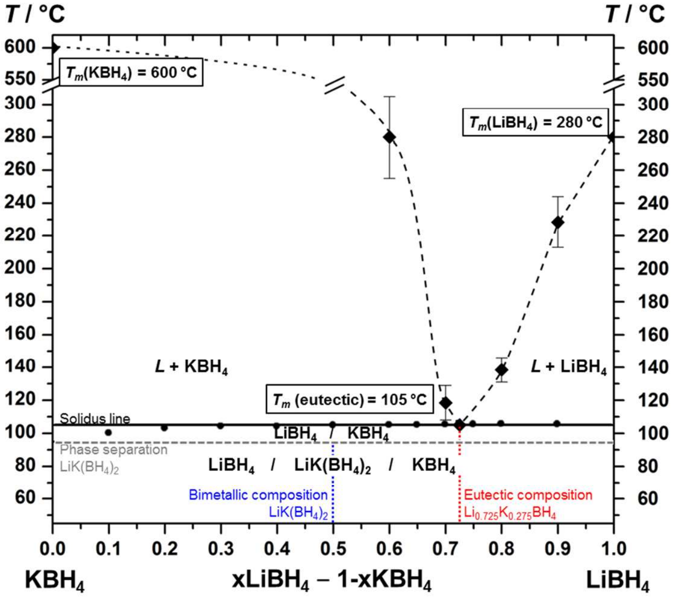

Figure 5 Binary phase diagram of the $LiBH_4$ – KBH_4 system. The eutectic composition and melting temperature were determined by DSC and *in situ* SR-PXD. The solidus temperatures were determined by DSC as the onset of the melting peak. The liquidus temperatures of $xLiBH_4$ – 1-$xKBH_4$ (x = 0.6 – 0.9, **s1-s4**) were estimated from TPPA studies and the uncertainty is indicated by the error bars. The liquidus line is a guide to the eye.

Formation of $LiK(BH_4)_2$ by mechanochemistry

In 2008, a bimetallic borohydride $LiK(BH_4)_2$ was synthesised by thermal treatment.[34] $LiK(BH_4)_2$ was reported to melt at 240 °C. This reported melting point may possibly correspond to the decreased melting point of the sample along the liquidus curves in the phase diagram, see Figure 5. Recently, $LiK(BH_4)_2$ was synthesised from mechano-chemistry as a by-product in a study of $KAl(BH_4)_4$.[35]

Since $LiK(BH_4)_2$ is already formed during manual grinding of the reactants $LiBH_4$ and KBH_4, mechano-chemical treatment was explored for the synthesis of $LiK(BH_4)_2$. The composition stoichiometrically corresponding to $LiK(BH_4)_2$, $0.5LiBH_4$–$0.5KBH_4$ (1:1, **s13**), and $0.665LiBH_4$–$0.335KBH_4$ (2:1, **s14**), which originally provided the highest yield of $LiK(BH_4)_2$,[34] were selected for a systematic sequential mechano-chemical investigation. Interestingly, $LiK(BH_4)_2$ is by PXD observed to form already after 5 min in both samples, indicating a partial reaction between $LiBH_4$ and KBH_4, see Figure 6 and S12. The diffracted intensity from $LiK(BH_4)_2$ (and small amounts of WC originating from the ball milling vial and balls) increases with increasing ball milling time. In **s13**, KBH_4 is the only reactant, which is visible in the PXD data after 24 and 36 h, see Figure 6. In sample **s14**, which is rich in $LiBH_4$, diffraction from $LiBH_4$ is visible after 36 h of ball milling. Weak diffraction from KBH_4 remains after 24 h of ball milling, but disappears at 36 h, see Figure S12.

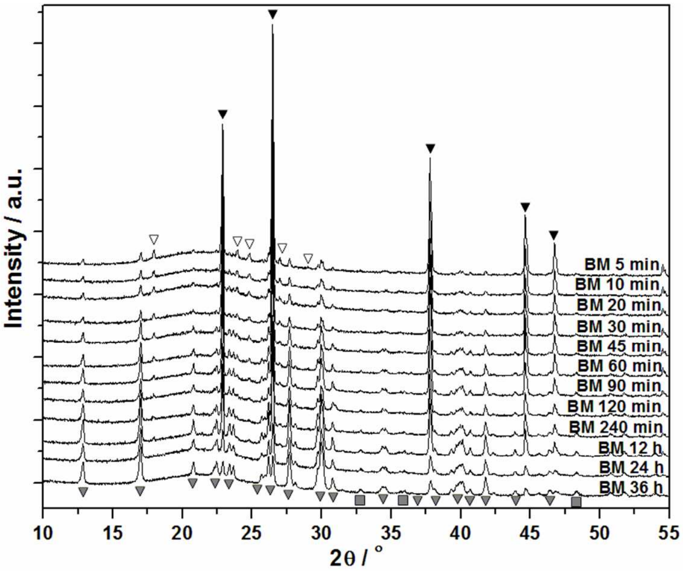

Figure 6 PXD patterns of $0.5LiBH_4$ – $0.5KBH_4$ (**s13**) ball milled to different extent up to 36 h (λ = 1.540593 Å). Symbols: white triangle $LiBH_4$, black triangle KBH_4, grey triangle $LiK(BH_4)_2$ and grey square WC.

$LiK(BH_4)_2$ is hence readily prepared by mechano-chemical methods, but prolonged ball milling is needed to complete the chemical reaction. One reason may be that the powder has a tendency to be compressed at the bottom of the vial at each opening of the ball milling vials, which could contribute to the long ball milling time needed to finish the chemical reaction. An excess of $LiBH_4$ is not necessary for the production of $LiK(BH_4)_2$ as previously suggested.[34] The fact that only excess KBH_4 is observed by PXD in **s13** after 36 h ball milling may be due to the weak X-ray scattering efficiency or amorphisation of lithium borohydride.[36,37]

Formation of $LiK(BH_4)_2$ by thermal treatment

To distinguish the effect of grinding or manual mixing from the effect of thermal treatment on the formation of $LiK(BH_4)_2$, we performed melting experiments in borosilicate capillaries for $0.5LiBH_4$ – $0.5KBH_4$ (**s5**) and $0.725LiBH_4$ – $0.275KBH_4$ (**s11**). After PXD analysis, the cooled capillary was crushed and repacked in a new capillary, in order to assess if slow cooling or hand mixing facilitates the formation of $LiK(BH_4)_2$, see Figure S13, S14 and S15. $LiK(BH_4)_2$ is not observed in **s5** or **s11** after melting and cooling showing that heat treatment is not responsible for the formation of $LiK(BH_4)_2$. After the heat treatment, melting and crushing of the sample, $LiK(BH_4)_2$ is observed in both **s5** and **s11**. The low diffracted intensity of the repacked sample may be due to contamination with crushed borosilicate glass. This experiment and the *in situ* melting experiment of **s12**, see Figure 4, indicates that the formation of $LiK(BH_4)_2$ is facilitated by physical pressure and not by heat treatment.

The unit cell parameters of $LiBH_4$, KBH_4 and $LiK(BH_4)_2$ were extracted by sequential Rietveld refinement of *in situ* SR-PXD data of **s12**, see Figure 4, between RT and 90 °C. The three compounds $LiBH_4$, KBH_4 and $LiK(BH_4)_2$ has the same number of formula units per unit cell, $Z = 4$, which means that the unit cell volumes are directly comparable.[28,34,38] The sum of unit cell volumes,

$\sum V = V_{LiBH4} + V_{KBH4}$, and the difference, $\Delta V = \sum V - V_{LiK(BH4)2}$, are shown in Figure 7. At room temperature, $\sum V$ is 28.8 ± 0.2 Å^3 larger than $V_{LiK(BH4)2}$. As the temperature increases to 90 °C, the bimetallic borohydride shows larger thermal expansion than the two monometallic compounds. This is illustrated by the decreasing volume difference ΔV from 28.8 ± 0.2 (T = 25 °C) to 23.1 ± 0.4 Å^3 (T = 90 °C). The smaller volume of $LiK(BH_4)_2$ compared to the added volume of $LiBH_4$ and KBH_4, $\sum V$, reveal a more dens $LiK(BH_4)_2$ structure, which indicates that $LiK(BH_4)_2$ is likely stabilised by pressure and not heat treatment leading to thermal expansion. This is in accord with the recent theoretical calculation suggesting that $LiK(BH_4)_2$ is metastable at ambient conditions, but stabilised by pressure.[31,32]

This work also illustrates, that new compounds prepared by mechano-chemistry in some cases can be considered metastable at ambient conditions, stabilised by pressure and may decompose to the reactants upon heating. The latter has previously been observed for the trimetallic borohydride $Li_3MgZn_5(BH_4)_{15}$, which decompose to mono and bi-metallic borohydrides at T = 120 C,[39] $NaK(BH_4)_2$, which dissociates into $NaBH_4$ and KBH_4 at room temperature[40] and $K_2Mg(BH_4)_4$, which dissociates into KBH_4 and $Mg(BH_4)_2$, at T = 300 °C.[41]

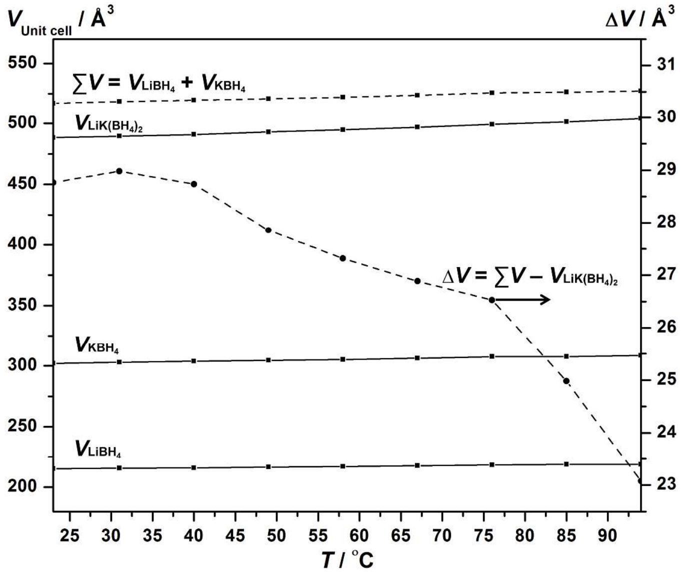

Figure 7 Unit cell volume of $LiBH_4$, KBH_4 and $LiK(BH_4)_2$ extracted from Rietveld refinement of *in situ* SR-PXD data of sample **s12**. The formula units per unit cell in $LiBH_4$, KBH_4 and $LiK(BH_4)_2$

are $Z = 4$. The sum of volumes $\sum V = V_{LiBH4} + V_{KBH4}$ and the difference $\Delta V = \sum V - V_{LiK(BH4)2}$ have been calculated. The standard deviation is less than 0.4 $Å^3$ on all the data points.

Conclusion

The eutectic composition for $xLiBH_4$ – $1-xKBH_4$ was determined to be x ~ 0.725 by a combination of differential scanning calorimetry, *in situ* SR-PXD and temperature programmed photographic analysis. This eutectic composition was found to melt at ~105 °C. This is the lowest melting point reported for a eutectic melting metal borohydride system, which may have properties similar to ionic liquids. This system may have a range of other interesting properties, e.g. as new fast ion conductors or as solvent or synthesis media for preparation and design of novel metal borohydrides or for hydrogen storage via new reactive hydride composites that take advantage of the low melting point and possible high reactivity. Eutectic metal borohydrides have the potential to be used as a liquid fuel with high energy density providing fast refueling of vehicles. The bimetallic $LiK(BH_4)_2$ is formed by hand mixing or ball milling of $LiBH_4$ and KBH_4 mixtures. However, the formation of $LiK(BH_4)_2$ does not require an excess of $LiBH_4$ or thermal annealing. The stability of $LiK(BH_4)_2$ appear to be governed by a decrease in unit cell volume as compared to the reactants. This work suggests that new compounds formed by mechano-chemistry may, in some cases, be considered metastable at ambient conditions, stabilised by pressure and may decompose to the reactants upon heating.

Acknowledgement

The work was supported by the Danish Council for Strategic Research, via the research project HyFillFast, the Danish National Research Foundation, Center for Materials Crystallography (DNRF93), and by the Danish Research Council for Nature and Universe (Danscatt). We acknowledge funding from the European Community's Seventh Framework Programme, The Fuel

Cells and Hydrogen Joint Undertaking (FCH JU), project BOR4STORE (303428). Part of this work was supported by the COST Action MP1103 "Nanostructured materials for solid-state hydrogen storage". The access to beamtime at the MAX-II synchrotron, Lund, Sweden in the research laboratory MAX-lab is gratefully acknowledged. We are grateful to the Carlsberg Foundation for support.

References

1. M. B. Ley, L. H. Jepsen, Y.-S. Lee, Y. W. Cho, J. M. Bellosta von Colbe, M. Dornheim, M. Rokni, J. O. Jensen, M. Sloth, Y. Filinchuk, J. E. Jørgensen, F. Besenbacher, and T. R. Jensen, *Mater. Today*, 2014, **17**, 122–128.

2. L. H. Jepsen, M. B. Ley, Y.-S. Lee, Y. W. Cho, M. Dornheim, J. O. Jensen, Y. Filinchuk, J. E. Jørgensen, F. Besenbacher, and T. R. Jensen, *Mater. Today*, 2014, **17**, 129–135.

3. M. Felderhoff, C. Weidenthaler, R. Helmolt, and U. Eberle, *Phys. Chem. Chem. Phys.*, 2007, **9**, 2643–2653.

4. J. M. Tarascon and M. Armand, *Nature*, 2001, **414**, 359–67.

5. M. Fichtner, *J. Alloys Compd.*, 2011, **509**, 529–534.

6. D. MacKay, *Sustainable Energy - without the hot air*, UIT Cambridge Ltd. Cambridge England, Cambridge, 3.5.2 edn., 2008.

7. A. Züttel, A. Borgschulte, and S. I. Orimo, *Scr. Mater.*, 2007, **56**, 823–828.

8. M. B. Ley, D. B. Ravnsbaek, Y. Filinchuk, Y.-S. Lee, R. Janot, Y. W. Cho, J. Skibsted, and T. R. Jensen, *Chem. Mater.*, 2012, **24**, 1654–1663.

9. M. B. Ley, S. Boulineau, R. Janot, Y. Filinchuk, and T. R. Jensen, *J. Phys. Chem. C*, 2012, **116**, 21267–21276.

10. M. Matsuo, Y. Nakamori, S. Orimo, H. Maekawa, and H. Takamura, *Appl. Phys. Lett.*, 2007, **91**, 224103–224103.

11. K. Takahashi, K. Hattori, T. Yamazaki, K. Takada, M. Matsuo, S. Orimo, H. Maekawa, and H. Takamura, *J. Power Sources*, 2013, **226**, 61–64.

12. S. Marks, J. G. Heck, M. H. Habicht, P. Oña-Burgos, C. Feldmann, and P. W. Roesky, *J. Am. Chem. Soc.*, 2012, **134**, 16983–6.

13. L. H. Rude, T. K. Nielsen, D. B. Ravnsbæk, U. Bösenberg, M. B. Ley, B. Richter, L. M. Arnbjerg, M. Dornheim, Y. Filinchuk, F. Besenbacher, and T. R. Jensen, *Phys. Status Solidi*, 2011, **208**, 1754–1773.

14. W. I. F. David, *Faraday Discuss.*, 2011, **151**, 399–414.

15. R. A. Varin, L. Zbroniec, M. Polanski, and J. Bystrzycki, *Energies*, 2010, **4**, 1–25.

16. A. Unemoto, M. Matsuo, and S. Orimo, *Adv. Funct. Mater.*, 2014, **24**, 2267–2279.

17. Y. Shang and R. Chen, *Energy & Fuels*, 2006, **20**, 2142–2148.

18. M. Paskevicius, M. P. Pitt, C. J. Webb, D. A. Sheppard, U. Filsø, E. M. Gray, and C. E. Buckley, *J. Phys. Chem. C*, 2012, **116**, 15231–15240.

19. R. M. Adams, in *Borax to Boranes*, American Chemical Society, 1961, vol. 32, pp. 60–68.

20. K. N. Semenenko, A. P. Chavgun, and V. N. Surov, *Russ. J. Inorg. Chem.*, 1971, **16**, 271–273.

21. M. Paskevicius, M. B. Ley, D. A. Sheppard, T. R. Jensen, and C. E. Buckley, *Phys. Chem. Chem. Phys.*, 2013, **15**, 19774–19789.

22. H. Hagemann, V. DAnna, J.-P. Rapin, R. Černý, Y. Filinchuk, K. C. Kim, D. S. Sholl, and S. F. Parker, *J. Alloys Compd.*, 2011, **509**, S688–S690.

23. E. G. Bardaji, Z. Zhao-Karger, N. Boucharat, A. Nale, M. J. van Setten, W. Lohstroh, E. Rohm, M. Catti, and M. Fichtner, *J. Phys. Chem. C*, 2011, **115**, 6095–6101.

24. Z. Zhao-Karger, R. Witter, E. G. Bardají, D. Wang, D. Cossement, and M. Fichtner, *J. Mater. Chem. A*, 2013, **1**, 3379.

25. J. Y. Lee, D. Ravnsbæk, Y.-S. Lee, Y. Kim, Y. Cerenius, J.-H. Shim, T. R. Jensen, N. H. Hur, and Y. W. Cho, *J. Phys. Chem. C*, 2009, **113**, 15080–15086.

26. H.-S. Lee, Y.-S. Lee, J.-Y. Suh, M. Kim, J.-S. Yu, and Y. W. Cho, *J. Phys. Chem. C*, 2011, **115**, 20027–20035.

27. A. Züttel, S. Rentsch, P. Fischer, P. Wenger, P. Sudan, P. Mauron, and C. Emmenegger, *J. Alloys Compd.*, 2003, **356-357**, 515–520.

28. J. Soulie, G. Renaudin, R. Erny, and K. Yvon, *J. Alloys Compd.*, 2002, **346**, 200–205.

29. E. M. Brown, *Introduction to Thermal Analysis: Techniques and Applications, Vol. 1.*, Kluwer Academic Publishers, Dordercht, 2001, 2001.

30. H. Oguchi, M. Matsuo, J. S. Hummelshøj, T. Vegge, J. K. Nørskov, T. Sato, Y. Miura, H. Takamura, H. Maekawa, and S. Orimo, *Appl. Phys. Lett.*, 2009, **94**, 141912 1–3.

31. K. C. Kim and D. S. Sholl, *J. Phys. Chem. C*, 2010, **114**, 678–686.

32. L. Tuan, C. K. Nguyen, and T. D. Huan, *Phys. status solidi*, 2014, **251**, 1539–1544.

33. G. J. Janz, *Molten Salts Handbook*, Academic Press, 1967.

34. E. A. Nickels, M. O. Jones, W. I. F. David, S. R. Johnson, R. L. Lowton, M. Sommariva, and P. P. Edwards, *Angew. Chem., Int. Ed.*, 2008, **47**, 2817–2819.

35. I. Dovgaliuk, V. Ban, Y. Sadikin, R. Černý, L. Aranda, N. Casati, M. Devillers, and Y. Filinchuk, *J. Phys. Chem. C*, 2013, **118**, 145–153.

36. M. Au, A. Jurgensen, and K. Zeigler, *J. Phys. Chem. B*, 2006, **110**, 26482–26487.

37. D. B. Ravnsbaek, Y. Filinchuk, R. Černý, M. B. Ley, D. Haase, H. J. Jakobsen, J. Skibsted, and T. R. Jensen, *Inorg. Chem.*, 2010, **49**, 3801–9.

38. S. C. Abrahams and J. Kalnajs, *J. Chem. Phys.*, 1954, **22**, 434.

39. R. Černý, P. Schouwink, Y. Sadikin, K. Stare, L. Smrčok, B. Richter, and T. R. Jensen, *Inorg. Chem.*, 2013, **52**, 9941–9947.

40. L. Seballos, J. Z. Zhang, E. Rönnebro, J. L. Herberg, and E. H. Majzoub, *J. Alloys Compd.*, 2009, **476**, 446–450.

41. P. Schouwink, V. D'Anna, M. B. Ley, L. M. Lawson Daku, B. Richter, T. R. Jensen, H. Hagemann, and R. Černý, *J. Phys. Chem. C*, 2012, **116**, 10829–10840.